ISSN 0915-633X

NATIONAL INSTITUTE FOR FUSION SCIENCE

Complexity in Laser Plasma Instabilities

M.M. Škorić, T. Sato, A. Maluckov and M.S. Jovanović

(Received - Nov. 15, 1999)

NIFS-618 Dec. 1999

This report was prepared as a preprint of work performed as a collaboration reserch of the National Institute for Fusion Science (NIFS) of Japan. This document is intended for infomation only and for future publication in a journal after some rearrangements of its contents.

Inquiries about copyright and reproduction should be addressed to the Research Information Center, National Institute for Fusion Science, Oroshi-cho, Toki-shi, Gifu-ken 509-02 Japan.

RESEARCH REPORT
NIFS Series

NAGOYA, JAPAN

General Invited Lecture delivered at the 24^{th} International Conference on Phenomena in Ionized Gases (*ICPIG*), Warsaw (Poland), 16-20 July 1999
– to appear in *Journal of Technical Physics* –

Complexity in Laser Plasma Instabilities

Miloš M. Škorić[(a)], Tetsuya Sato[(b)], Aleksandra Maluckov[(c)] and Moma S. Jovanović[(d)]

[a)] *Vinča Institute of Nuclear Sciences P.O.B. 522, 11001 Belgrade, Yugoslavia*
[b)] *Theory and Computer Simulation Center, National Institute for Fusion Science, Toki 509-5292, Japan*
[c)] *The Graduate Institute for Advanced Studies, Hayama, Kanagawa 240-01, Japan*
[d)] *Department of Physics, Faculty of Sciences, University of Niš, P.O.B. 91, 18001 Niš, Yugoslavia*

Abstract

High intensity laser interaction with a plasma exhibits a rich variety of strongly nonlinear plasma phenomena. In an underdense plasma, stimulated Raman scattering (*SRS*) and stimulated Brillouin scattering (*SBS*) are two laser parametric instabilities of a greatest relevance. We show examples of isolated nonlinear *SRS* and *SBS* and discuss some of the experimental *SRS* anomalies that largely depart from the standard theory. As an example of a complex interplay between nonlinear *SRS* and *SBS* we show results of their anti-correlated behavior. Based on a concept of self-organization we put forward a simple model of *SRS* capable of reproducing basic experimentally observed anomalous features. Finally, we close with an example of fascinating new physics observed in *SRS* induced by an ultra-short pulse relativistic-intensity laser.

KEYWORDS: ICF, Laser plasmas, Stimulated Raman and Brillouin scattering, Self-Organization

1 Introduction

Laser plasma interactions are a useful model for exploring strongly nonlinear plasma phenomena. In particular, high intensity laser coupling with a hot plasma exhibits various nonlinear plasma processes including laser parametric instabilities. In laser driven inertial confinement fusion (*ICF*) research, great concern is related to nonlinear laser parametric instabilities operating in an underdense plasma; such as, stimulated Brillouin scattering (*SBS*) and stimulated Raman scattering (*SRS*) [1, 2]. Stimulated scattering of laser light apart from an undesirable energy loss frequently produces hot electrons that can pre-heat the *ICF* target. It is a purpose of this lecture to review some of complex and highly nonlinear laser plasma phenomena related to scattering of laser light in a plasma. It is this physical situation where observed anomalous features point out to an inadequacy of standard linear alike theories [1, 2, 3].

Firstly, we shall focus on examples of isolated nonlinear *SBS* and *SRS* plasma processes. Further, we point out that certain experimentally observed anomalies could possibly result from a complex interplay of two and more coexisting nonlinear plasma instabilities. In particular, we discuss the question of self-consistency in plasma modeling and coexistence and interplay between nonlinear stimulated Brillouin and Raman scattering. The term Complexity in a more rigorous sense denotes evolution of highly nonlinear far from equilibrium systems exhibiting instabilities, structural bifurcation and self-organization to complex ordered states [4]. Following the concept of self-organization, we put forward a simple self-consistent model of stimulated Raman scattering, capable of producing basic anomalous features similar to those observed in high intensity laser plasma experiments [5, 6].

2 Stimulated Raman and Stimulated Brillouin Scattering

Parametric instabilities are of a great concern in the high-intensity laser-plasma interaction experiments ($I > 10^{15}$ W/cm^2) since they can produce reflection and scattering of incoming laser light and generate hot electrons [1, 2].

Laser driven parametric instabilities were first considered for gases. However, it appears that the self-consistent electric fields created by charged particles in a plasma lead to more complex behavior than in gases and solids. More precisely, parametric instabilities are due to laser light wave coupling with normal modes of the medium. The normal modes in a plasma are either low frequency electrostatic waves, the ion sound waves, or high frequency electrostatic waves, the electron plasma (Langmuir) waves. A parametric coupling between three or more waves can occur when momentum and energy matching conditions are satisfied (vide infra).

Further, we concentrate on stimulated Brillouin scattering instability and stimulated Raman instability because these are the two most important instabilities in the underdense- coronal plasma and of basic relevance to the coupling of laser energy to a target. *SBS* is the parametric decay of the incoming laser light into another laser light wave and an ion sound wave. This process can occur at any plasma density below critical density (the density where the laser frequency equals local electron plasma frequency) and is weakly sensitive to the density non-uniformity. *SRS*, on the other hand, is the decay of the incoming laser light into second light wave and a Langmuir (electron plasma) wave. It takes place below the quarter of the critical density, first as an absolute instability while at lower densities *SRS* turns into a convective instability. Below critical density several other parametric instabilities can also exist, such as, e.g., Langmuir decay instability, two-plasmon decay instability and filamentation instability (see Fig. 1). Each instability is limited by the dispersion relation and the frequency and wavenumber matching conditions. Initially, most of the theory has been addressing the linear behavior of laser parametric instabilities. Typically, instability threshold and exponential growth rate in weak and strong coupling limits were analytically calculated for various parametric processes [1, 2]. However, it appeared that in most experiments, these instabilities are almost always in a nonlinear state [7]. Moreover, it often happens that laser parametric instabilities saturate through strongly nonlinear regimes that correspond to large amplitude waves leading to plasma heating through wavebreaking and electron trapping [2].

3 Anomalous Regimes of SRS

Extensive experimental studies of nonlinear stimulated Raman backscattering have been followed by analytics, fluid and particle simulations [6, 2, 1]. In a strongly driven case, Raman instability exponentiates until arrested by nonlinear and dissipative effects. The saturation comes, basically, through pump depletion and/or higher order nonlinearities as well as kinetic dissipation related to electron trapping and Langmuir wave breaking [1, 2]. While pump depletion is readily included in fluid modeling, the latter effects are inherently kinetic. However, after more than two decades of intensive particle simulation studies, nonlinear Raman scattering is understood to posses relatively clear, albeit anomalous overall features [2]. Suppression of *SRS* is highly desirable in connection with a need to reduce hot electron generation. Indeed, correlation between hot electron generation and *SRS* was found in many experiments. A primary source for hot electron generation is understood to be due to large amplitude Langmuir waves excited in a plasma. In Fig. 2 the fraction of the laser energy in hot (supra-thermal) electrons was plotted versus the measured fraction of the energy of Raman scattered laser light [7]. Excellent correlation has also been found in temporally resolved data.

As a result of electron trapping and breaking of large Langmuir waves a hot tail-suprathermal electron population is generated. The corresponding velocity of hot (fast) electrons roughly equals the phase velocity of the electron plasma wave. As a general feature, two temperature (Maxwellian-like) electron distribution is recorded, for the thermal (bulk) and suprathermal (hot tail) electrons. Energy exchange leads to an increase of the bulk temperature at the expense of plasma wave dissipation. However, actual details of this complex scenario are determined by wave turbulence and the electron transport, both influenced strongly by boundary and other plasma conditions. Thus, qualitative understanding of anomalous Raman features has enabled useful scaling relations and semi-empirical formulae, typically extracted from the averaged (time and shot) short-run data. Generally taken, a realistic long time saturation (e.g. >10,000 plasma wave periods) does not appear to be assessable to even high performance particle simulation due to required computer time and limitations of the numerical scheme involving large number of particles

[2, 8]. It is this situation that has motivated us to address a problem of anomalous Raman in a long time evolution. In the last section, we study a SRS saturation to self-organizing plasma states using a general concept of complexity in plasmas in a system open to an environment [5]. Accordingly, we develop a phenomenological hybrid kinetic-fluid model to try to emulate basic physics of anomalous Raman as a precursor to state-of-the-art particle simulation with open boundaries [9], planned for the future.

4 Interplay between Laser Plasma Instabilities

The interaction of laser light and different plasma modes that takes place in the coronal plasma often do not appear in isolation, and consequently a rich interplay between laser plasma instabilities is observed [3]. Of particular importance is the interaction between two scattering instabilities: stimulated Raman and stimulated Brillouin instability For those plasma parameters of interest to ICF, it was found that SRS and SBS can coexist over large underdense plasma regions, while their growth and saturation my be affected by each other. On the other hand, a simultaneous presence of SRS and SBS suggests the possibility for various couplings between Langmuir and ion sound waves. We discuss simple examples of direct and indirect interplay between SRS and SBS and consider their effect which can invalidate scaling to experiments using linear instability growth rate .

The first experimental observation of competition between stimulated Brillouin and stimulated Raman scattering was reported in early eighties [10]. When the temporal evolution of SRS and SBS light was compared, a strong correlation was observed between saturation level of SRS, and the level of SBS light. In a preformed plasma, driven with 1 nsec CO_2 laser pulse, direct observation of Langmuir waves associated with SRS and ion waves related to SBS was made possible. An early quenching of SRS by SBS produced ion sound waves was found (see Fig. 3). The Langmuir waves were observed only during the early part of the laser pulse, and disappeared coincidental with the onset of ion sound wave driven by SBS [10].

An attempt was made to examine a possibility to suppress stimulated Raman and Brillouin scattering by increasing a collisionality of a plasma. Indeed for SRS, collisional suppression has been demonstrated, as it appears that large enough electron-ion collision rate could strongly damp SRS driven Langmuir wave to effectively halt the instability growth We show the fraction of the laser energy that was Raman scattered in disk experiments. plotted in Fig 4 versus estimated value of the collision frequency to the instability growth rate [11]. The Raman reflectivity drops strongly around theoretically predicted value of the collision over growth rate close to 0.3. It also appears plausible to expect regimes with suppressed stimulated Brillouin scattering by increasing the ion sound damping. A direct way to enhance ion damping is to increase Landau damping by changing plasma composition to include protons. As expected, a reduction of SBS was observed in early CO_2 laser experiments, as well as in recent gas bag and toroidal hohlraum targets using Nova laser [3]. However, rather unexpectedly , novel regimes are also found where larger ion wave damping enhances the stimulated Raman scattering [3]. It turned out, that even if the linear growth rate of SRS is independent of ion sound damping the saturation level of SRS driven Langmuir wave can depend on the secondary parametric process. Namely, the so called Langmuir decay instability which is the Langmuir decay into another Langmuir plus ion sound wave has a threshold proportional to both electron and ion damping rates. For larger ion damping the threshold is higher, leading to higher electron density fluctuation and higher reflectivity of saturated SRS. Indeed, an increase of SRS with ion sound damping observed in recent gas bag experiments is shown in Fig.5 . The ion damping was varied by changing the proton impurity fraction. A regime is clearly seen where SRS reflectivity in creases with damping [12]. The early time results correspond to higher temperatures. Indeed, in this novel nonlinear regime one finds that SRS and SBS appear to be anti-correlated.

Further, we stress the importance of self-consistent calculations based on the correct zero-order plasma state [3]. Recently, it was pointed out that in laser produced plasmas, the electron velocity distribution can be rather different from Maxwellian, even if effect of induced plasma waves is neglected. The usual Maxwellian velocity distribution is the special case with $n = 2$ power in the exponent, while higher n's correspond to the so-called, super Gaussian distributions which are depleted in high energy electrons. A number of effects can modify the electron distribution. For example, collisional absorption (inverse Bremsstrahlung) preferentially heats slower, more collisional electrons. Therefore, when the rate of electron heating is greater than the rate at which they are equilibrated, the heated distribution function becomes super Gaussian. More generally, nonlocal transport results in distribution functions with n larger than 2 ;while at high intensities one finds super Gaussian distributions with n as large as 5. Modified electron distributions can result in many important effects, ranging from changes in instability thresholds and growth rates to variations in the atomic physics [3].

5 Self-organization of Saturated SRS

A) Background

Self–organization (*SO*) is a generic process which describes a spontaneous formation of an ordered structure in a nonlinear far-from equilibrium system. Energy pumping, nonlinear instability, entropy production and expulsion are key governing processes. An open system was found to exhibit different features in *SO*, depending on whether the energy pumping is instantaneous—final state of minimum energy, or continuous—the dynamical state of intermittency [4, 5].

In this section, an attempt is made to study kinetic self-organization through a process of stimulated Raman backscattering (*SRBS*) in an underdense plasma [6]. As described, stimulated Raman scattering is a resonant three-wave (3WI) parametric instability which corresponds to the decay of an incident electromagnetic pump wave into a scattered wave plus an electron plasma wave (EPW). Important effects, especially in the context of laser–fusion [2], are input energy loss, plasma heating and generation of suprathermal (hot) electrons. However, to account for these effects, kinetic treatment of highly nonlinear electron interaction with EPW is required. To emulate these effects we apply a hybrid three–wave phenomenological kinetic model of *SRBS*, recently proposed by Škorić et al. [13]. We focus at dissipative structures that evolve at plasma micro- and macro-scales and attempt to relate entropy rate extrema to structural transitions between different states of *SO*.The basic theoretical facts about hybrid model are shown in the second part. Characteristic numerical results in the context of *SO* are exposed in the third and fourth part of this section.

B) A Hybrid model

The basic equations are coupled three–wave equations [1] for Slowly varying complex amplitudes of a pump (a_0), backscattered wave (a_1) and *EPW* (a_2), respectively :

$$\frac{\partial a_0}{\partial t} + V_0 \frac{\partial a_0}{\partial x} = -a_1 a_2 \,,$$
$$\frac{\partial a_1}{\partial t} - V_1 \frac{\partial a_1}{\partial x} = a_0 a_2^* \,, \tag{1}$$
$$\frac{\partial a_2}{\partial t} + V_2 \frac{\partial a_2}{\partial x} + \Gamma a_2 + i\sigma |a_2|^2 a_2 = \beta_0^2 a_0 a_1^* \,.$$

The wave–particle interaction [2] is modeled by a damping term in the *EPW* equation of (1), Γa_2 which includes a phenomenological anomalous kinetic dissipation and entropy balance related to a kinetic self-organization. Parameter Γ consists of: collisional damping (Γ_{coll}), 'linear' (Landau) damping by hot — resonant electrons ($\gamma_l \sim n_h$), where $n_h(t)$ stands for spatially averaged hot electron density:

$$\frac{dn_h(t)}{dt} = \frac{n_b(L,t)}{L} \int_{v_h - v_{tr}(L,t)}^{v_h + v_{tr}(L,t)} v f_b dv - a \frac{v_h(t) n_h(t)}{L} \,, \tag{2}$$

(n_b is bulk electron density, f_b is bulk distribution function, v_h is velocity of hot electrons which equals the *EPW* phase velocity, v_{tr} is trapping velocity and a is particle transport parameter), and nonlinear damping due to trapped resonant bulk electrons (in the thermal Maxwellian):

$$2\gamma_{nl} W(t) = \frac{m n_b(L,t)}{2L} \int_{v_h - v_{tr}(L,t)}^{v_h + v_{tr}(L,t)} v^3 f_b(v) dv \,, \tag{3}$$

where $W(t)$ is spatially averaged *EPW* energy.

Open boundaries and reemittance of fresh ambient electrons [9] is assumed. The particles (bulk and hot electrons) and energy (wave and particle) are being exchanged between a plasma and an environment through open boundaries with a conservation of particle number and total energy in the system. Accordingly, heat balance equation (effect of plasma heating; E_b, E_h and $S_{tot} \to S_b + S_h + S_q$ are the average bulk and hot electron energy or corresponding energy flux of the bulk, hot and return ambient electrons, respectively) takes a form:

$$\frac{dW(t)}{dt} = \frac{d(E_b(t) + E_h(t))}{dt} + k \cdot S_{tot} \Big|_0^L \,. \tag{4}$$

C) Simulation

The simulation is made via central–difference numerical code [6], which is complemented by equations for generation of resonant electrons (2) and heat balance equation (4) in the wave–particle system.

Parameters are: $n_0 = 0.1n_{cr}$, $T_{b0} = 0.5keV$ and pump intensity, $\beta_0 = 0.0253$. Openness of a system, k (0-1) was chosen as a bifurcation parameter. The effect of self-organization at large (wave-fluid) macro-scales is illustrated in Fig. 6. Depending on k the system shows characteristic features of different dynamical regimes: steady–state ($k = 0.007$), quasi-periodic ($k = 0.05$), periodic ($k = 0.5$) and intermittent regime ($k > 0.9$).

Fig. 7 illustrates the micro-scale (kinetic) self-organization via temporal evolution of the electron distribution function. In the treatment bi–Maxwellian (bulk–hot) electron distribution, as suggested by kinetic and particle–in–cell (PIC) simulations [2, 8], was assumed One can readily observe an essential connection and interplay between two levels of SO in a dissipative plasma.

D) Dissipative structures and entropy rate

Self-organization in a strongly nonlinear far-from-equilibrium system leads to a creation of ordered states that reflect an interaction of this system with its environment. These novel dynamical structures or patterns, named dissipative structures to stress the crucial role of dissipation in their creation, have become a central theme of the science of complexity [5, 6, 13]. On the other hand, there is a fundamental role of the entropy, in particular, the rate of entropy change in an open system [4]. The rate of entropy production and its removal basically governs self-organization features of a system. A large amount of effort has been spent in attempts to relate the entropy rate extrema to structural bifurcations and transitions between different ordered states [5, 6].

First, we focus at self-organized dissipative structures developed at the macro-scale. Indeed, in our model, basic wave and fluid density variables were assumed to vary slowly in space-time. Therefore, we expect that original spatio-temporal profiles, found in simulations, should correspond to large dissipative structures, self-organized at macro-scale levels. As an illustration, we plot the plasma wave profiles (Fig. 8), in particular, to reveal a genuine spatio-temporal nature of an intermittent regime as compared to regular dynamical regimes of the steady-state and quasi-periodic type [2, 13]. Spatio-temporal complexity of quasi-steady and travelling wave patterns with regular and chaotic features is found in different states of self-organization.

Further, in Fig. 9 we plot the entropy rate $dS(t)/dt$ in time together with a spatio-temporal profile of the scattered wave energy. We calculate the entropy S related to distributions $F_i = n_i f_i$, as: $S(t) = S_b(t) + S_h(t)$, where

$$S_i(t) = -\int_0^L dx \int_{-\infty}^{\infty} dv\, F_i\,(x,v,t)\ln F_i\,(x,v,t).$$

where $i = b, h$.

For an intermittent regime, featuring an interchange between chaotic and laminar phases, we find a clear evidence of structural transitions corresponding to the maximum (positive) and minimum (negative) entropy rate. As a striking example of self-organization in an open system we find a rapid entropy jump which coincides with an onset of a chaotic phase. Subsequent anomalous dissipation and entropy growth is halted by a sudden entropy expulsion into the environment. Negative burst in entropy rate indicates a bifurcation from a chaotic, back to a laminar quasi-periodic phase. An intermittent nature of this regime is shown through a repetitive pattern of behavior. We note that complex dissipative wave structures are mapped onto a more simple entropy rate time series. Intervals of near zero entropy rate during a laminar phase, mean a net balance between the entropy production and its expulsion. This serves as a possible example of a stationary nonequilibrium state realized in a strongly nonlinear open system [5].

Moreover, a hybrid nature of our model also allows us to recover kinetic properties of self-organization. By using an analytical dependence of the electron distribution on varying hot (bulk) temperature and density we expose a genuine picture of kinetic self-organization at plasma micro-scales. To show the self-organization featuring micro-levels, we plot the electron velocity distribution function. In Fig. 7 we see a three-dimensional view of the electron velocity distribution in time for different saturated Raman regimes, as indicated by values of parameter k. Kinetic self-organization of varying complexity is revealed in thermal and suprathermal (hot) regions of the electron distribution. In Fig. 10, we further plot the electron distribution in time versus the entropy rate related to an intermittent regime. Once again, an evidence of micro-scale structural transitions that correspond to entropy rate extrema, is found. Indeed, one is able to observe a complex connection and interplay between macro and micro levels of self-organization in an open dissipative plasma.

E) Conclusions

In conclusion, we believe that our findings appear to be a first indication of a generic intermittent scenario in a kinetic self-organization of anomalous Raman instability. At this point we may note that one is able to claim a consistency with the working hypothesis and general scenario of self-organization in plasmas [5, 13]. As a further step, we expect an important justification of our hybrid -modeling of saturated Raman complexity by the novel open boundary particle simulation code, currently under development [9]. As an early illustration, we show in Fig. 11, recent particle-in-cell simulation data for a model of an isolated plasma slab in a vacuum [8]. For same plasma parameters, particle simulations (Fig. 11) show an evident support of above Raman reflectivity pattern (Fig. 6, right top), obtained for a closed ($k = 0.007$) system.

6 Summary

In this paper we have addressed some important examples of a complex plasma behavior related to nonlinear *SRS* and *SBS* instabilities. As an introduction we have discussed nonlinear saturation of the isolated Raman and Brillouin scattering in laser plasmas. Understanding the nonlinear saturation of *SRS* and *SBS* is critical for the success of laser fusion with targets designed to achieve ignition; such as those currently proposed for the National Ignition Facility (NIF) [16]. We point out the failure of standard nonlinear parametric theory to reproduce experimentally observed *SRS* anomalies. As an example of a complex interplay we show data on coexisting and anti-correlated *SRS* and *SBS*. Applying the general concept of self-organization, for the first time to *SRS*, we have constructed a simple but powerful 3WI model for anomalous *SRS* evolution that shows consistency with particle simulations.

Finally, we turn to an example of fascinating new physics that was recently observed as one moved into a regime of collective effects in plasmas induced by ultra-short pulse ultra-high intensity ($I > 10^{18}$ W/cm^2) laser. A Livermore-UCLA collaboration has observed a subpicosecond version of classic laser plasma stimulated Raman backscatter [14]. The backscattered light displays anomalous spectral signatures that strongly depend on laser intensity. Broad and modulated frequency spectrum that spreads to the blue side of the standard Raman shifted line, that is obviously different from classic *SRS*, was typically observed (see Fig. 12). The use of prepulse did not significantly affect the modulation, hence ruling out the ionization as a probable cause. More recently similar results were reported by Rutherford, Limeil and Livermore groups. Above spectral anomalies were recovered and explained in the framework of a simple theoretical 3WI fluid model of *SRS*, by these authors [6]. It was shown in this model [6, 13] that backscatter complexities, modulated and incoherently broadened spectra follow a quasi-periodic and intermitent route to chaos (vide supra), while a spectral blue shift was attributed to a relativistic decrease of plasma frequency. These findings were reinforced by results obtained by $1\frac{2}{2}$-dimensional, fully relativistic particle in cell simulations [8].

Acknowledgements

This work was supported in parts by the Ministry of Science and Technology of the Republic of Serbia, Project-01E11.

References

[1] D.W. Forslund, J.M. Kindel, E.L. Lindman, *Phys. Fluids* **18** (1975) 1002.

[2] W. L. Kruer, *The Physics of Laser Plasma Interactions*, Addison, N. Y. (1988); ibid., *Phys. Fluids* **B** (19 91) 2356.

[3] W. L. Kruer, B. B. Afeyan, A. E. Chou, R. K. Kirkwood, D. S. Montgomery, P .W. Rambo, S. C. Wilks, *Phys. Scripta* **T75** (1998) 7. and references therein

[4] G. Nicolis and I. Prigogine, *Exploring Complexity*, Freeman, N. Y. (1989)

[5] T. Sato and the Complexity Simulation Group, *Phys. Plasmas* **3** (1996) 261.

[6] M. M. Škorić, M. S. Jovanović, M. Rajković, *Phys. Rev. E* **53** (1996) 4056.; *Europhys. Lett.* **34** (1996) 19.

[7] R. P. Drake, R. E. Turner, B. F. Lasinski, K. G. Estabrook, E. M. Campbell, C. L. Wang, D. W. Phillion, E. A. Williams, W. L. Kruer, *Phys. Rev. Lett.* **53** (1984) 1739.

[8] S. Miyamoto, K. Mima, M. Škorić, M. S. Jovanović, *J. Phys. Soc. Jap.* **67** (1998) 1281.

[9] H. Takamaru, T. Sato, R. Horiuchi, K. Watanabe and Complexity Simulation Group, *J. Phys. Soc. Jap.* **66** (1997) 3826.

[10] H. A. Baldis, D. M. Villeneuve, C. Labaune, D. Pesme, W. Rozmus. W. L. Kruer, P. E. Young, *Phys. Fluids* **B3** (1991) 2341.

[11] R. P. Drake, *Comments Plasma Phys. Controlled Fusion* **12** (1989) 181.

[12] R. E Kirkwood, B.J. MacGowan, D S. Montgomery, B.B. Afeyan, W.L Kruer, J.D. Moddy, K.G Estabrook, C.A. Back, S.H. Glenzer. M.A. Blain, E.A. Williams, R.L. Berger, B F. Lasinski, *Phys.Rev. Lett.* **77** (1996) 2706.

[13] M. M. Škorić, T Sato, A. Maluckov, M. S. Jovanović, *NIFS Report*, No. 549 (1998); *Phys. Review E.*, to appear.

[14] C. J. Joshi, P. B. Corkum *Phys. Today* **48** (1995) 36.

[15] C. A. Coverdale, C.B. Darrow, C.D. Decker, N.M. Naumova, T.Zh Esirkepov, A.S. Sakharov, S.V. Bulanov, W.B. Mori, K.C. Tzeng, *Plasma Phys. Reports* **22** (1996) 685.

[16] D.S. Montgomery, B.B. Afeyan, J.A. Cobble, J.C. Fernandez, M. D. Wilke, S.H. Glenzer, R.K. Kirkwood, B.J. MacGowan, J.D. Moody, E.L. Lindman, D.H. Munro, B.H. Wilde, H.A. Rose, D.F. Dubois, B. Bezzerides, H.X. Vu, *Phys. Plasmas* **5** (1998) 1973.

Figure captions

Fig. 1. Regions of underdense (corona) plasma where various laser instabilities can exist.

Fig. 2. The fraction of laser energy in hot (supra-thermal) electrons as inferred from hard x-rays versus the measured fraction of energy in Raman backscattered light; after [7].

Fig. 3. Levels of ion sound waves from *SBS* and Langmuir waves from *SRS* obtained by Thomson scattering in a preformed plasma with a CO_2 laser. The Langmuir waves due to *SRS* were observed only during an early time and disappeared coincidental with the ion sound waves driven by *SBS*; after [10].

Fig. 4. The measured fraction of the light Raman scattered from Au disks versus estimated ratio of the electron-ion collision frequency to the *SRS* growth rate. The disks were irradiated with 0.3 microns laser light at various intensities; after [11].

Fig. 5. *SRS* reflectivity measured with gas bag targets versus the proton impurity fraction and normalized ion sound damping; after [12, 3]. A novel regime in which *SRS* reflectivity increases with ion sound damping is evident.

Fig. 6. Density of hot electrons and reflectivity versus time $[\omega_0^{-1}]$ for $k = 0.007$, 0.05, 0.5, 0.9 (top to bottom), respectively.

Fig. 7. Three-dimensional view of the electron velocity distrubution in time for different saturated Raman regimes, as indicated by values of parameter k. Micro-kinetic scale self-organization of varying complexity is revealed in both thermal and suprathermal (hot) regions of the electron distribution.

Fig. 8. Spatio-temporal profile of the electron plasma wave for varying k values. Different dissipative structures are seen on the route to complexity, from the steady-state via quasi-periodic to intermittent regimes.

Fig. 9. Intermittent dissipative backscatter-wave structures versus the corresponding entropy rate in time. Positive entropy jump coincides with an onset of chaos, while a negative burst indicates a transition from a chaotic to a laminar phase of *SO* at macro-scales.

Fig. 10. Intermittent electron distribution versus the entropy rate in time. Similar to Fig. 9, structural bifurcations at micro-scales, correspond to entropy rate extrema.

Fig. 11. Simulation data for Raman reflectivity in time, obtained by an one-and-two-halves electromagnetic, relativistic, particle-in-cell code. (after [8]). Initial plasma parameters were the same as above, with a pump equal to 0.02.

Fig. 12. Spectra of backscattered light as a function of laser pulse intensity demonstrating a transition from classic *SRS* to anomalous backscattering; after [15]; and private communication

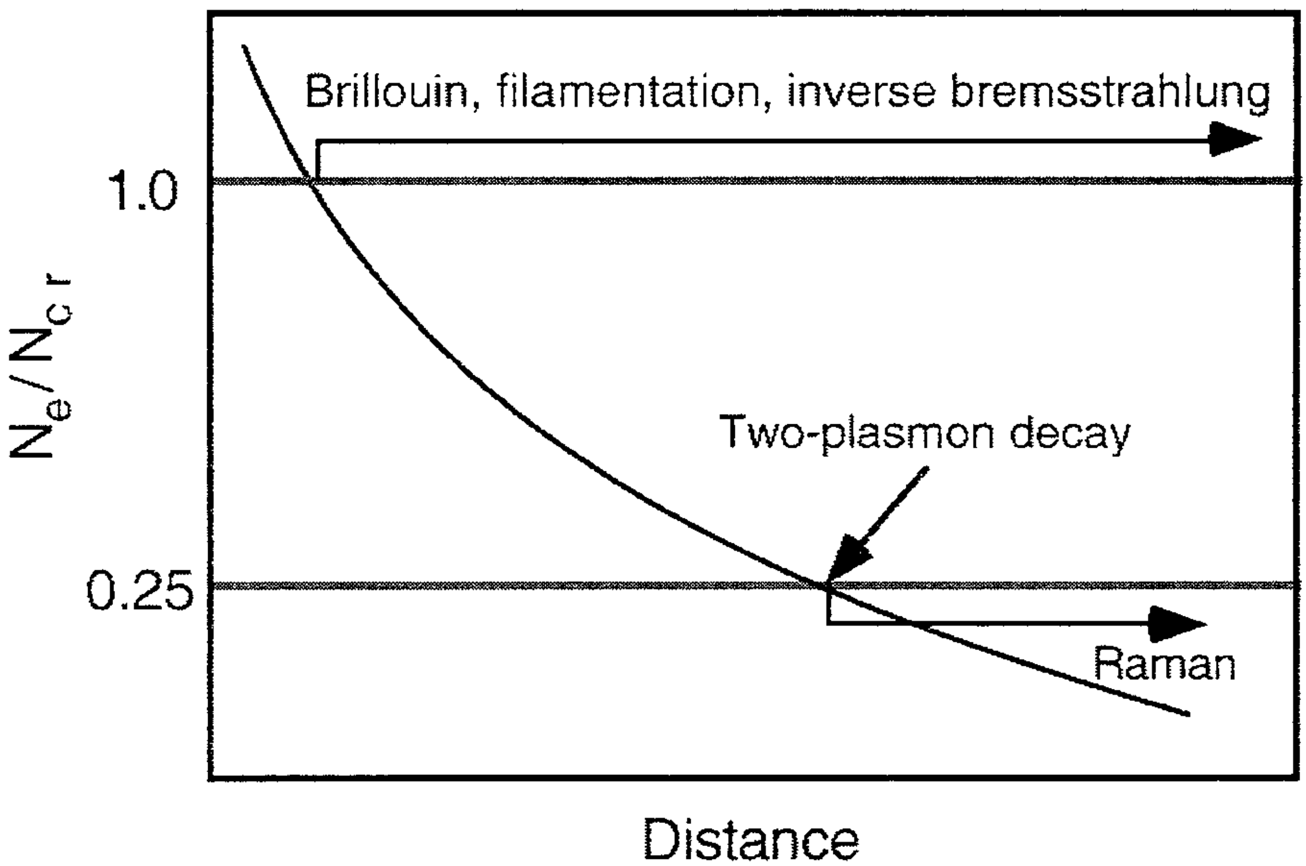

Brillouin, filamentation, inverse bremsstrahlung
1.0
N_e/N_{cr}
Two-plasmon decay
0.25
Raman
Distance

Fig.1

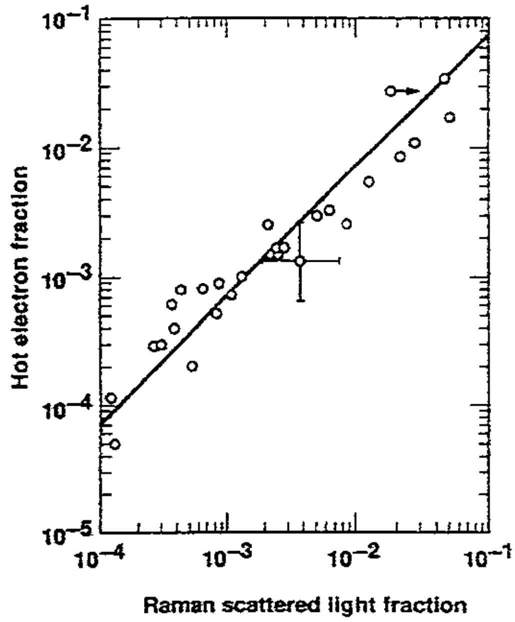

Hot electron fraction
Raman scattered light fraction
10^{-1}
10^{-2}
10^{-3}
10^{-4}
10^{-5}
10^{-4}
10^{-3}
10^{-2}
10^{-1}

Fig.2

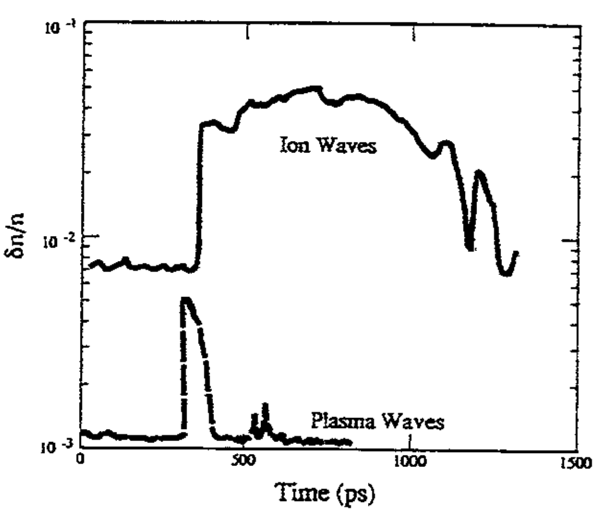

δn/n
Ion Waves
Plasma Waves
Time (ps)
10^{-1}
10^{-2}
10^{-3}
0
500
1000
1500

Fig.3

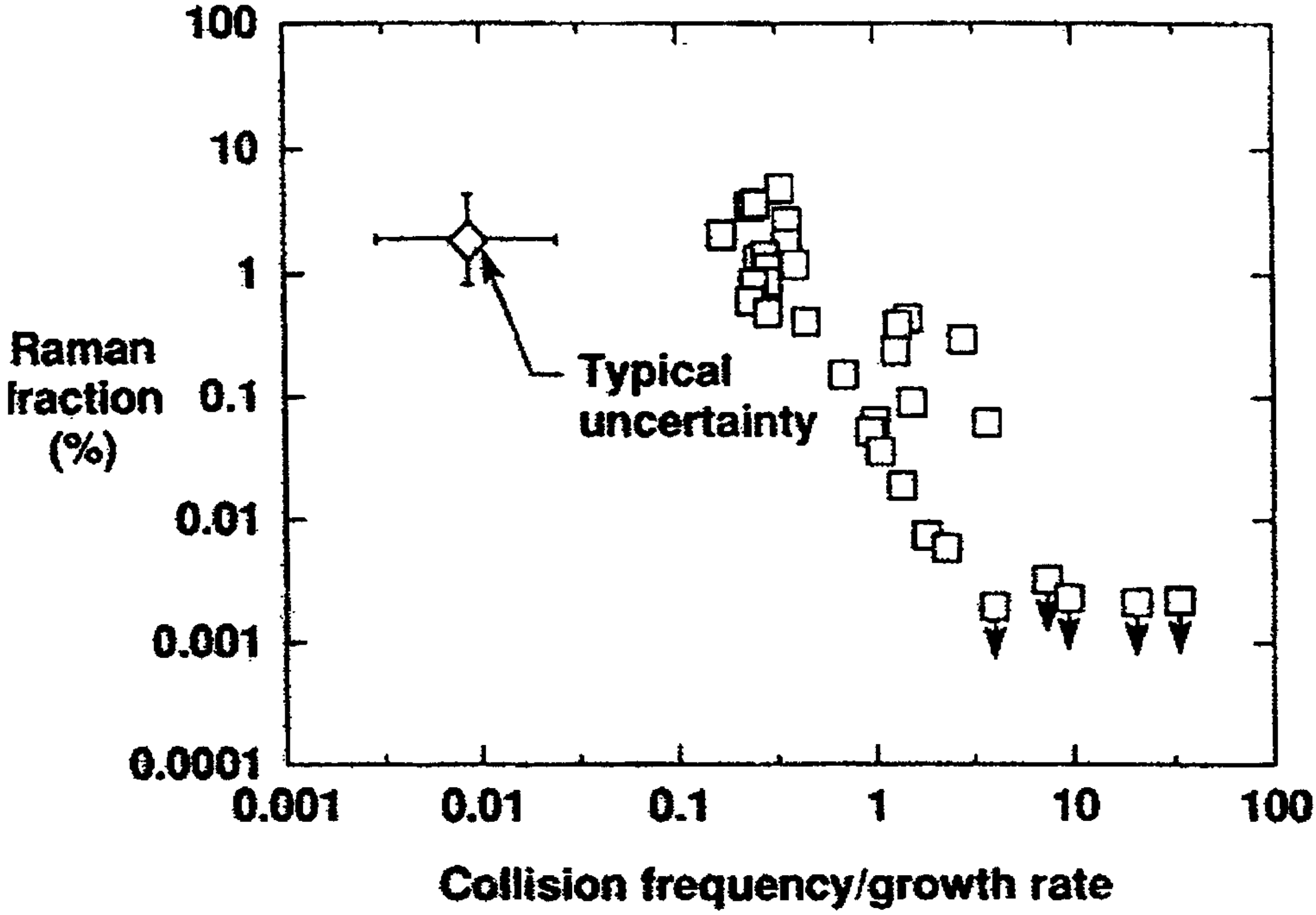

100
10
1
Raman
fraction
(%)
0.1
0.01
0.001
0.0001
Typical
uncertainty
0.001
0.01
0.1
1
10
100
Collision frequency/growth rate

Fig.4

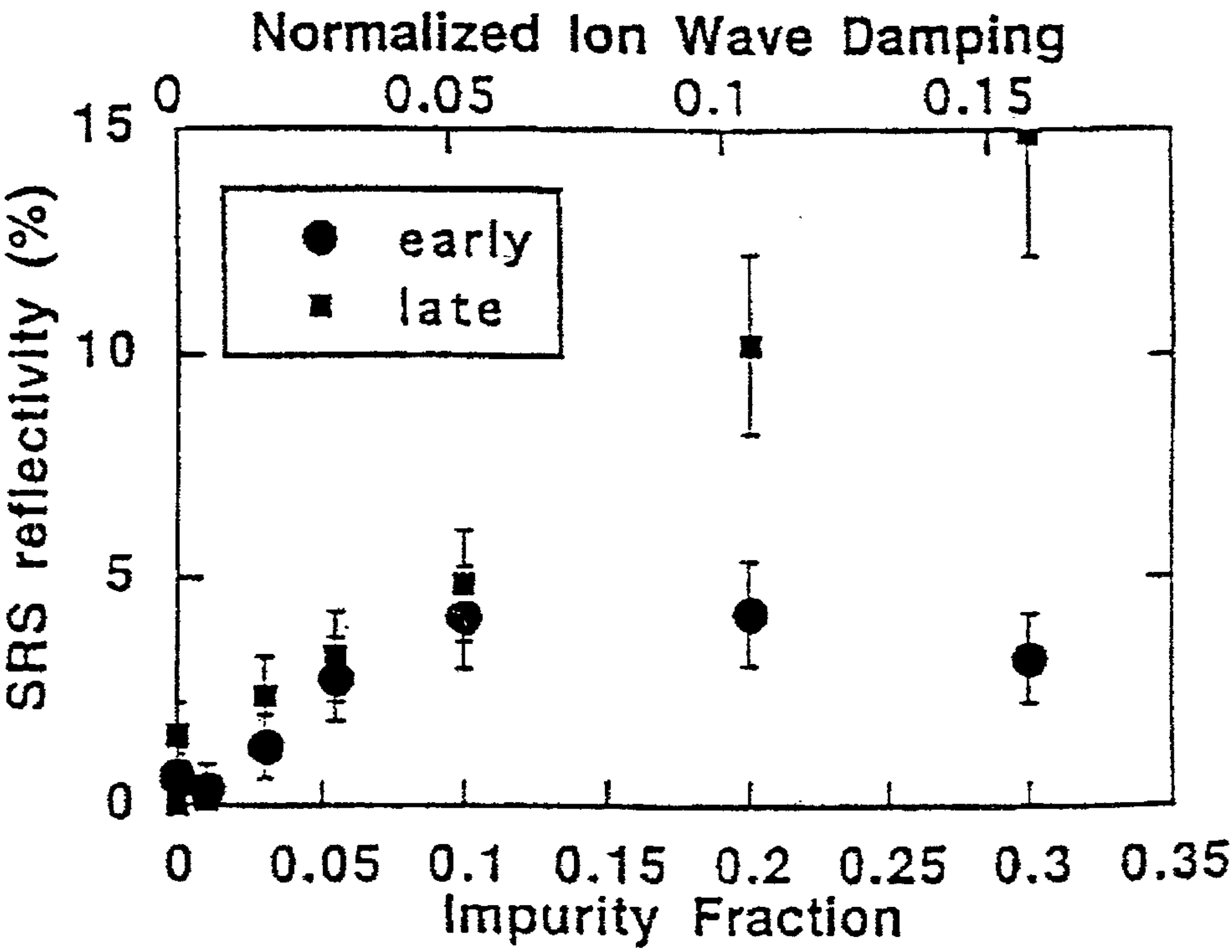

Normalized Ion Wave Damping
0
0.05
0.1
0.15
15
10
5
0
early
late
SRS reflectivity (%)
0
0.05
0.1
0.15
0.2
0.25
0.3
0.35
Impurity Fraction

Fig.5

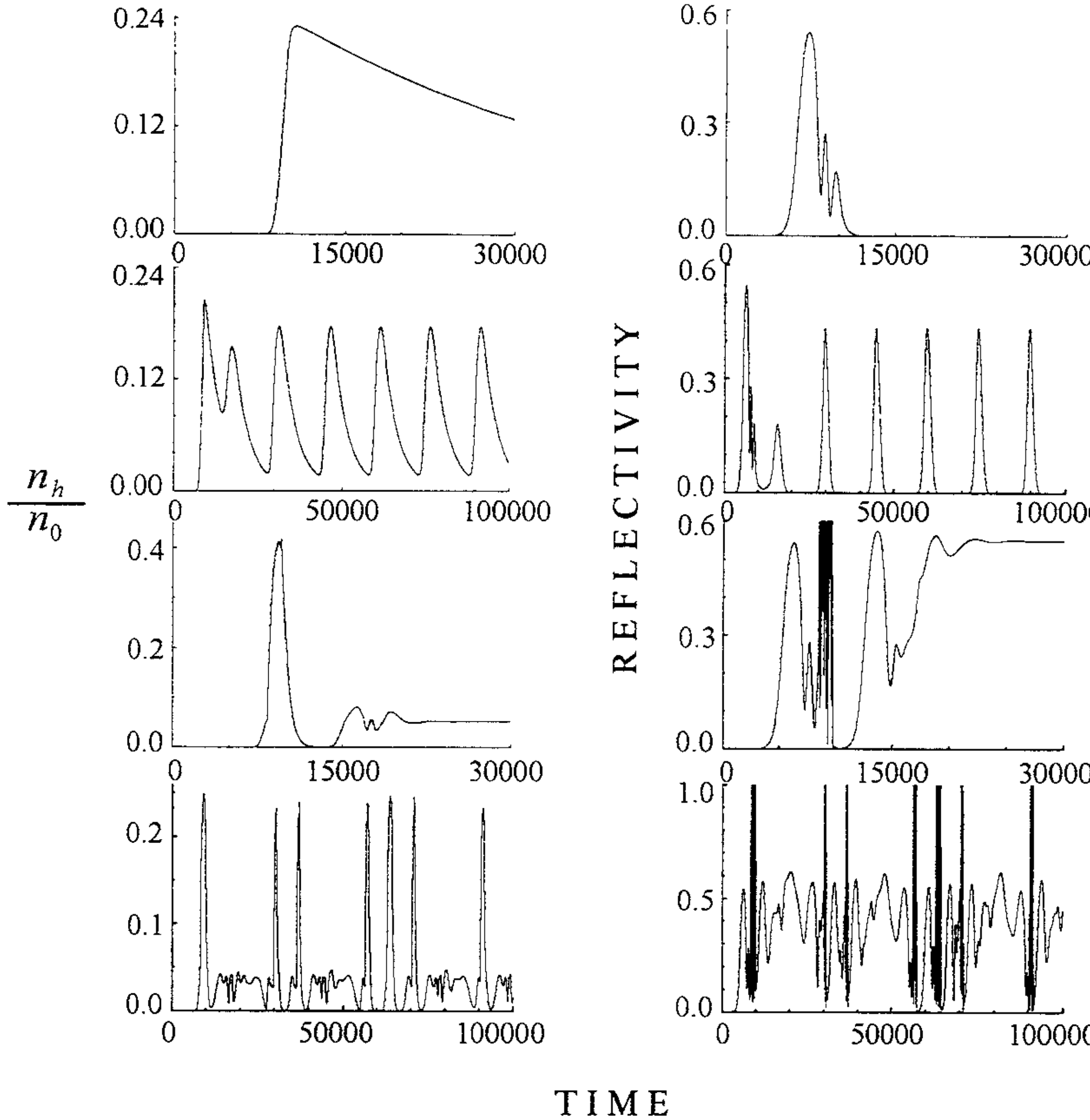

0.24
0.12
0.00
0
15000
30000
0.6
0.3
0.0
0
15000
30000
0.24
0.12
0.00
0
50000
100000
0.6
0.3
0.0
0
50000
100000
$\frac{n_h}{n_0}$
REFLECTIVITY
0.4
0.2
0.0
0
15000
30000
0.6
0.3
0.0
0
15000
30000
0.2
0.1
0.0
0
50000
100000
1.0
0.5
0.0
0
50000
100000
TIME

Fig.6

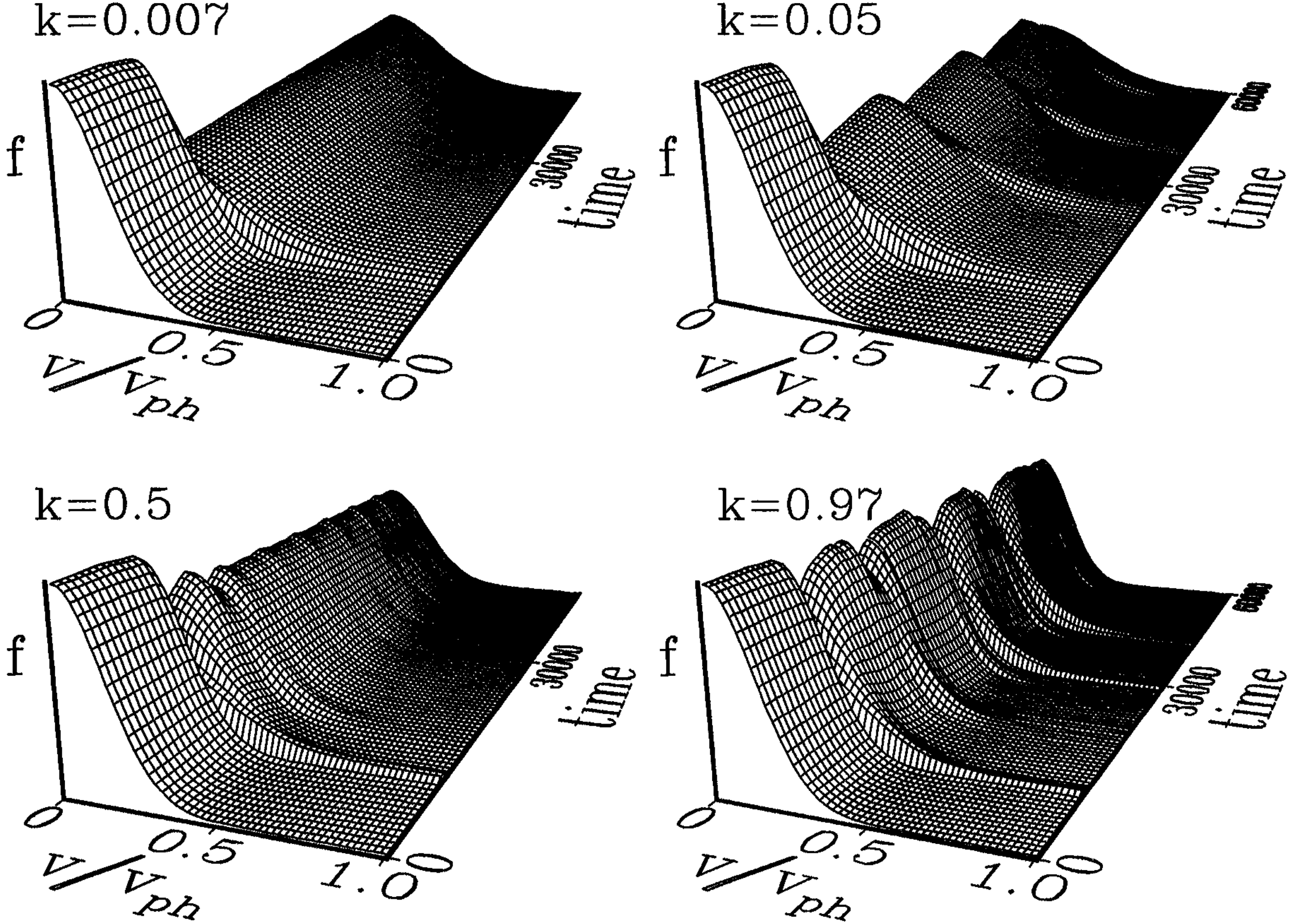

Fig.7

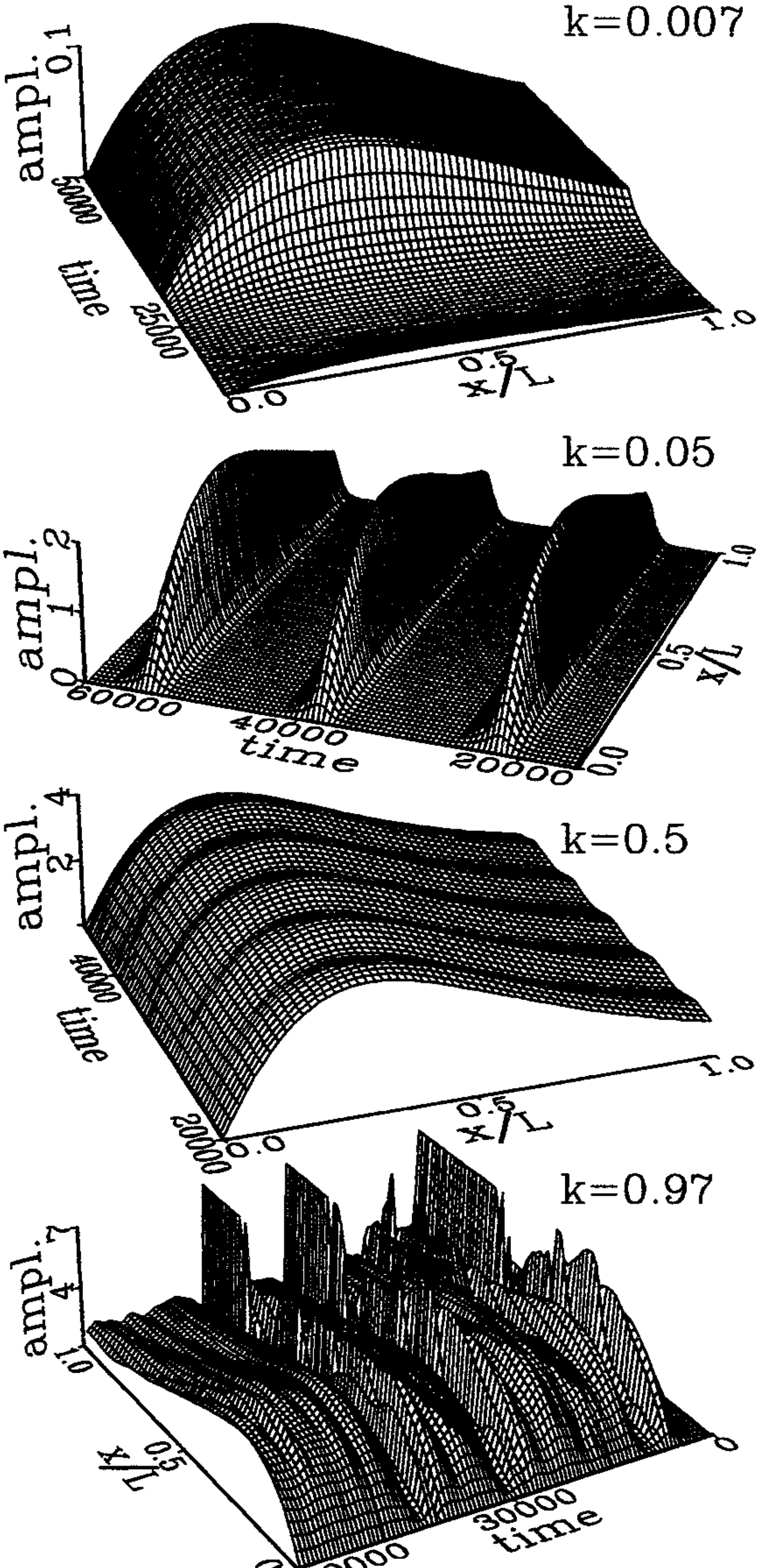

k=0.007
ampl.
0.1
time
25000
x/L
0.0
0.5
1.0
k=0.05
ampl.
2
1
0
60000
40000
time
20000
x/L
0.0
0.5
1.0
k=0.5
ampl.
4
2
40000
time
20000
x/L
0.0
0.5
1.0
k=0.97
ampl.
7
4
1.0
x/L
0.5
0.0
60000
30000
time
0

Fig.8

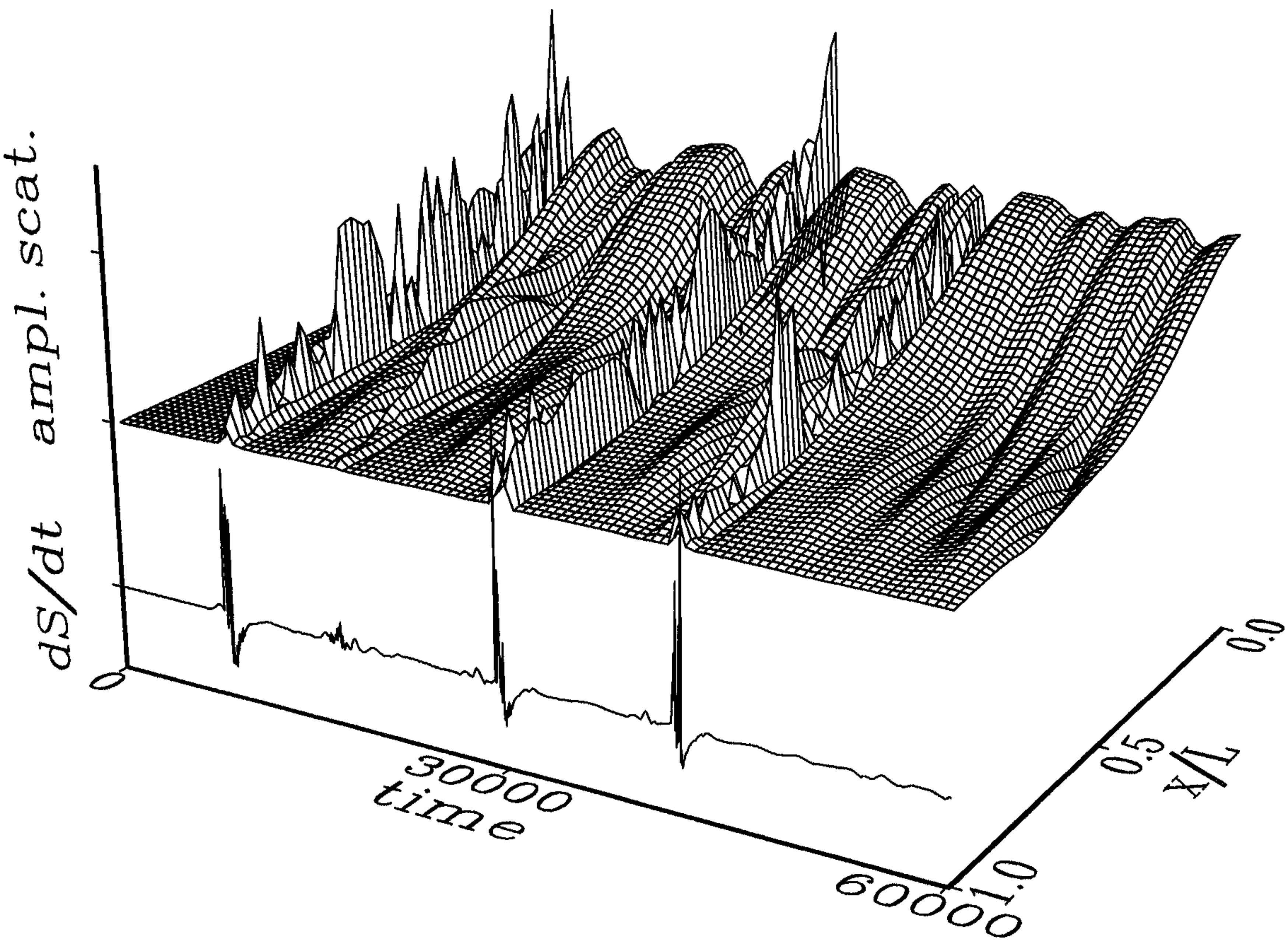

Fig.9

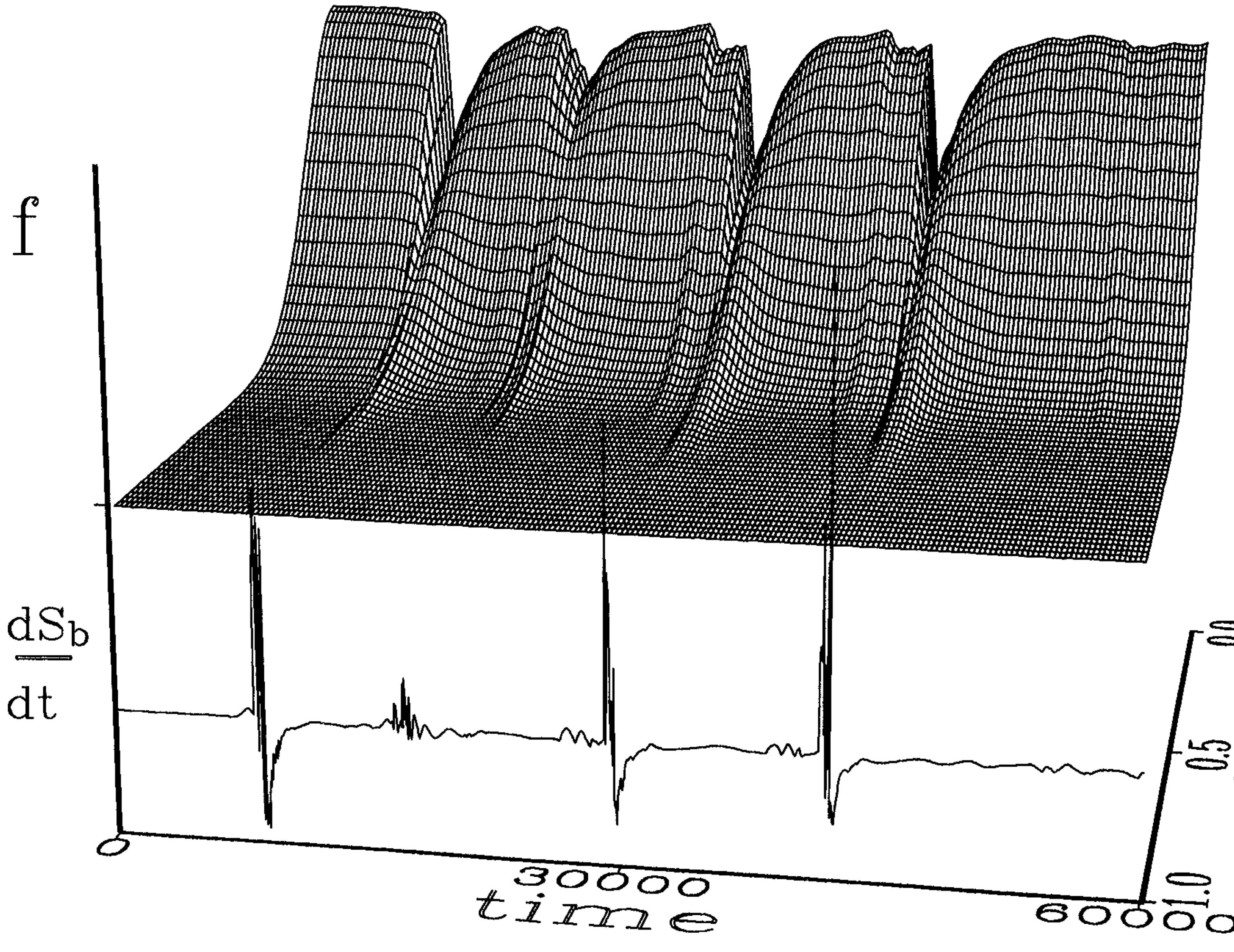

Fig.10

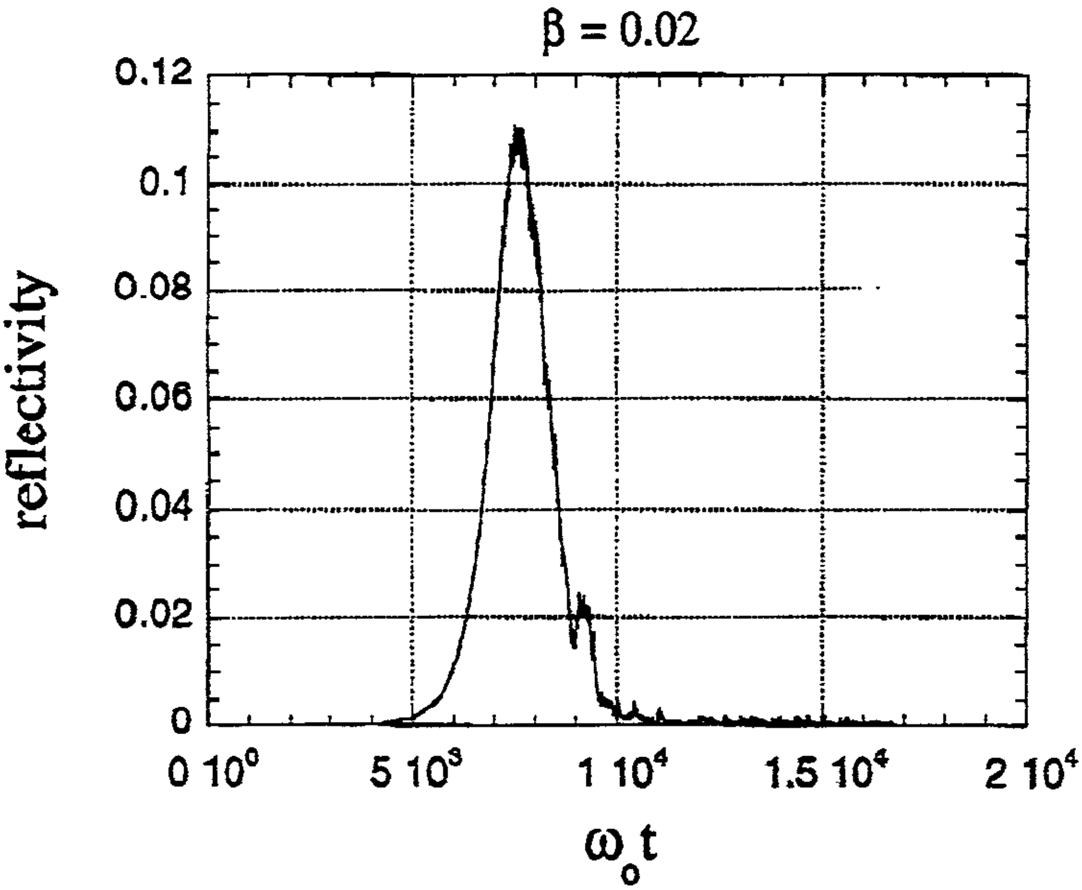

β = 0.02
reflectivity
0.12
0.1
0.08
0.06
0.04
0.02
0
0 10⁰
5 10³
1 10⁴
1.5 10⁴
2 10⁴
ω₀t

Fig.11

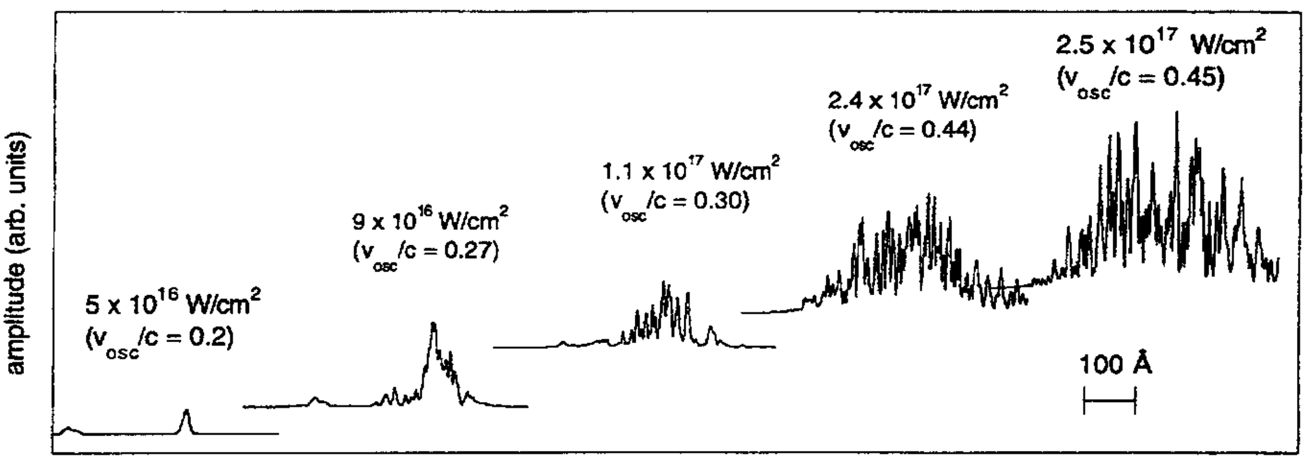
amplitude (arb. units)
5 x 10^16 W/cm^2
(v_osc/c = 0.2)
9 x 10^16 W/cm^2
(v_osc/c = 0.27)
1.1 x 10^17 W/cm^2
(v_osc/c = 0.30)
2.4 x 10^17 W/cm^2
(v_osc/c = 0.44)
2.5 x 10^17 W/cm^2
(v_osc/c = 0.45)
100 Å

Fig.12

Recent Issues of NIFS Series

NIFS-555 H Nakamura, K Ikeda and S Yamaguchi,
Physical Model of Nernst Element, Aug. 1998

NIFS-556 H Okumura, S Yamaguchi, H. Nakamura, K. Ikeda and K Sawada,
Numerical Computation of Thermoelectric and Thermomagnetic Effects, Aug 1998

NIFS-557 Y Takeiri, M Osakabe, K. Tsumori, Y. Oka, O Kaneko, E Asano, T Kawamoto, R Akiyama and M Tanaka,
Development of a High-Current Hydrogen-Negative Ion Source for LHD-NBI System, Aug.1998

NIFS-558 M. Tanaka, A Yu Grosberg and T Tanaka,
Molecular Dynamics of Structure Organization of Polyampholytes, Sep 1998

NIFS-559 R. Horiuchi, K. Nishimura and T. Watanabe,
Kinetic Stabilization of Tilt Disruption in Field-Reversed Configurations, Sep 1998
(IAEA-CN-69/THP1/11)

NIFS-560 S. Sudo, K Kholopenkov, K. Matsuoka, S. Okamura, C. Takahashi, R Akiyama, A Fujisawa, K Ida, H Idei, H Iguchi, M. Isobe, S Kado, K. Kondo, S Kubo, H. Kuramoto, T. Minami, S. Morita, S. Nishimura, M. Osakabe, M Sasao, B Peterson, K. Tanaka, K Toi and Y. Yoshimura,
Particle Transport Study with Tracer-Encapsulated Solid Pellet Injection, Oct 1998
(IAEA-CN-69/EXP1/18)

NIFS-561 A Fujisawa, H. Iguchi, S. Lee, K Tanaka, T. Minami, Y. Yoshimura, M. Osakabe, K Matsuoka, S Okamura, H. Idei, S Kubo, S. Ohdachi, S. Morita, R. Akiyama, K. Toi, H. Sanuki, K. Itoh, K. Ida, A Shimizu, S. Takagi, C Takahashi, M Kojima, S Hidekuma, S Nishimura, M Isobe, A. Ejiri, N. Inoue, R Sakamoto, Y Hamada and M Fujiwara,
Dynamic Behavior Associated with Electric Field Transitions in CHS Heliotron/Torsatron, Oct 1998
(IAEA-CN-69/EX5/1)

NIFS-562 S. Yoshikawa,
Next Generation Toroidal Devices; Oct 1998

NIFS-563 Y. Todo and T. Sato,
Kinetic-Magnetohydrodynamic Simulation Study of Fast Ions and Toroidal Alfvén Eigenmodes; Oct 1998
(IAEA-CN-69/THP2/22)

NIFS-564 T. Watari, T. Shimozuma, Y. Takeiri, R. Kumazawa, T. Mutoh, M. Sato, O. Kaneko, K. Ohkubo, S. Kubo, H. Idei, Y. Oka, M. Osakabe, T. Seki, K. Tsumori, Y. Yoshimura, R. Akiyama, T Kawamoto, S. Kobayashi, F Shimpo, Y Takita, E Asano, S Itoh, G Nomura, T. Ido, M. Hamabe, M. Fujiwara, A. Iiyoshi, S. Morimoto, T Bigelow and Y.P. Zhao,
Steady State Heating Technology Development for LHD; Oct 1998
(IAEA-CN-69/FTP/21)

NIFS-565 A. Sagara, K.Y. Watanabe, K. Yamazaki, O Motojima, M Fujiwara, O Mitarai, S Imagawa, H Yamanishi, H Chikaraishi, A Kohyama, H. Matsui, T. Muroga, T. Noda, N. Ohyabu, T Satow, A.A. Shishkin, S Tanaka, T Terai and T. Uda,
LHD-Type Compact Helical Reactors, Oct 1998
(IAEA-CN-69/FTP/03(R)

NIFS-566 N. Nakajima, J. Chen, K. Ichiguchi and M. Okamoto,
Global Mode Analysis of Ideal MHD Modes in L=2 Heliotron/Torsatron Systems; Oct 1998
(IAEA-CN-69/THP1/08)

NIFS-567 K Ida, M Osakabe, K Tanaka, T Minami, S Nishimura, S Okamura, A Fujisawa, Y Yoshimura, S Kubo, R. Akiyama, D.S.Darrow, H Idei, H. Iguchi, M. Isobe, S. Kado, T. Kondo, S. Lee, K Matsuoka, S Morita, I Nomura, S. Ohdachi, M Sasao, A Shimizu, K. Tumori, S. Takayama, M. Takechi, S. Takagi, C. Takahashi, K Toi and T Watari,
Transition from L Mode to High Ion Temperature Mode in CHS Heliotron/Torsatron Plasmas; Oct 1998
(IAEA-CN-69/EX2/2)

NIFS-568 S Okamura, K Matsuoka, R. Akiyama, D.S. Darrow, A Ejiri, A Fujisawa, M Fujiwara, M Goto, K Ida H Idei, H Iguchi, N Inoue, M. Isobe, K. Itoh, S. Kado, K. Khlopenkov, T. Kondo, S. Kubo, A Lazaros, S Lee, G Matsunaga, T Minami, S. Morita, S Murakami, N Nakajima, N. Nikai, S. Nishimura, I. Nomura, S Ohdachi, K. Ohkuni, M Osakabe, R Pavlichenko, B Peterson, R. Sakamoto, H. Sanuki, M. Sasao, A. Shimizu, Y. Shirai, S. Sudo, S Takagi, C Takahashi, S Takayama, M. Takechi, K Tanaka, K. Toi, K. Yamazaki, Y. Yoshimura and T Watari,
Confinement Physics Study in a Small Low-Aspect-Ratio Helical Device CHS, Oct 1998
(IAEA-CN-69/OV4/5)

NIFS-569 M.M Skoric, T Sato, A. Maluckov, M S. Jovanovic,
Micro- and Macro-scale Self-organization in a Dissipative Plasma, Oct 1998

NIFS-570 T Hayashi, N Mizuguchi, T-H. Watanabe, T Sato and the Complexity Simulation Group,

Nonlinear Simulations of Internal Reconnection Event in Spherical Tokamak; Oct. 1998
(IAEA-CN-69/TH3/3)

NIFS-571 A. Iiyoshi, A. Komori, A. Ejiri, M. Emoto, H. Funaba, M. Goto, K. Ida, H. Idei, S. Inagaki, S. Kado, O Kaneko, K. Kawahata, S. Kubo, R. Kumazawa, S. Masuzaki, T. Minami, J. Miyazawa, T. Morisaki, S. Morita, S. Murakami, S. Muto, T. Muto, Y. Nagayama, Y. Nakamura, H. Nakanishi, K. Narihara, K. Nishimura, N. Noda, T. Kobuchi, S. Ohdachi, N. Ohyabu, Y. Oka, M. Osakabe, T. Ozaki, B.J. Peterson, A. Sagara, S. Sakakibara, R. Sakamoto, H. Sasao, M. Sasao, K. Sato, M. Sato, T. Seki, T. Shimozuma, M. Shoji, H. Suzuki, Y. Takeiri, K. Tanaka, K. Toi, T. Tokuzawa, K. Tsumori, I. Yamada, H. Yamada, S. Yamaguchi, M. Yokoyama, K.Y.Watanabe, T. Watari, R. Akiyama, H. Chikaraishi, K. Haba, S. Hamaguchi, S. Iima, S. Imagawa, N. Inoue, K Iwamoto, S. Kitagawa, Y. Kubota, J. Kodaira, R. Maekawa, T. Mito. T. Nagasaka, A. Nishimura, Y. Takita, C. Takahashi, K. Takahata, K. Yamauchi, H. Tamura, T. Tsuzuki, S. Yamada, N. Yanagi, H. Yonezu, Y. Hamada, K. Matsuoka, K. Murai, K. Ohkubo, I Ohtake, M. Okamoto, S. Sato, T. Satow, S. Sudo, S. Tanahashi, K. Yamazaki, M. Fujiwara and O. Motojima,
An Overview of the Large Helical Device Project; Oct. 1998
(IAEA-CN-69/OV1/4)

NIFS-572 M. Fujiwara, H. Yamada, A. Ejiri, M. Emoto, H. Funaba, M. Goto, K. Ida, H. Idei, S. Inagaki, S. Kado, O. Kaneko, K. Kawahata, A. Komori, S Kubo, R. Kumazawa, S. Masuzaki, T. Minami, J. Miyazawa, T. Morisaki, S. Morita, S. Murakami, S. Muto, T Muto, Y. Nagayama, Y. Nakamura, H. Nakanishi, K. Narihara, K. Nishimura, N. Noda, T. Kobuchi, S. Ohdachi, N. Ohyabu, Y. Oka, M. Osakabe, T. Ozaki, B. J. Peterson, A. Sagara, S. Sakakibara, R. Sakamoto, H. Sasao, M. Sasao, K. Sato, M. Sato, T. Seki, T. Shimozuma, M. Shoji, H. Sazuki, Y. Takeiri, K. Tanaka, K. Toi, T. Tokuzawa, K. Tsumori, I. Yamada, S. Yamaguchi, M. Yokoyama, K.Y. Watanabe, T. Watari, R. Akiyama, H. Chikaraishi, K. Haba, S. Hamaguchi, M. Iima, S. Imagawa, N. Inoue, K. Iwamoto, S. Kitagawa, Y. Kubota, J. Kodaira, R. Maekawa, T. Mito, T. Nagasaka, A. Nishimura, Y. Takita, C. Takahashi, K. Takahata, K. Yamauchi, H. Tamura, T. Tsuzuki, S. Yamada, N. Yanagi, H. Yonezu, Y. Hamada, K. Matsuoka, K. Murai, K. Ohkubo, I. Ohtake, M. Okamoto, S. Sato, T. Satow, S. Sudo, S. Tanahashi, K. Yamazaki, O. Motojima and A. Iiyoshi,
Plasma Confinement Studies in LHD; Oct. 1998
(IAEA-CN-69/EX2/3)

NIFS-573 O. Motojima, K. Akaishi, H. Chikaraishi, H. Funaba, S. Hamaguchi, S. Imagawa, S. Inagaki, N. Inoue, A. Iwamoto, S. Kitagawa, A. Komori, Y. Kubota, R. Maekawa, S. Masuzaki, T. Mito, J. Miyazawa, T. Morisaki, T. Muroga, T. Nagasaka, Y. Nakmura, A. Nishimura, K. Nishimura, N. Noda, N. Ohyabu, S. Sagara, S. Sakakibara, R. Sakamoto, S. Satoh, T. Satow, M. Shoji, H. Suzuki, K. Takahata, H. Tamura, K. Watanabe, H. Yamada, S. Yamada, S. Yamaguchi, K. Yamazaki, N. Yanagi, T Baba, H. Hayashi, M. Iima, T. Inoue, S. Kato, T. Kato, T. Kondo, S. Moriuchi, H. Ogawa, I Ohtake, K. Ooba, H. Sekiguchi, N. Suzuki, S. Takami, Y. Taniguchi, T. Tsuzuki, N. Yamamoto, K. Yasui, H. Yonezu, M. Fujiwara and A. Iiyoshi,
Progress Summary of LHD Engineering Design and Construction; Oct. 1998
(IAEA-CN-69/FT2/1)

NIFS-574 K. Toi, M. Takechi, S. Takagi, G. Matsunaga, M. Isobe, T. Kondo, M. Sasao, D.S. Darrow, K. Ohkuni, S. Ohdachi, R Akiyama A. Fujisawa, M. Gotoh, H. Idei, K. Ida, H. Iguchi, S. Kado, M. Kojima, S. Kubo, S. Lee, K. Matsuoka, T. Minami, S. Morita, N. Nikai, S. Nishimura, S. Okamura, M. Osakabe, A. Shimizu, Y. Shirai, C. Takahashi, K. Tanaka, T. Watari and Y. Yoshimura,
Global MHD Modes Excited by Energetic Ions in Heliotron/Torsatron Plasmas; Oct. 1998
(IAEA-CN-69/EXP1/19)

NIFS-575 Y. Hamada, A. Nishizawa, Y. Kawasumi, A. Fujisawa, M. Kojima, K. Narihara, K. Ida, A. Ejiri, S. Ohdachi, K. Kawahata, K. Toi, K. Sato, T. Seki, H. Iguchi, K. Adachi, S. Hidekuma, S.Hirokura, K. Iwasaki, T. Ido, R. Kumazawa, H. Kuramoto, T. Minami, I.. Nomura, M. Sasao, K.N. Sato, T. Tsuzuki, I. Yamada and T. Watari,
Potential Turbulence in Tokamak Plasmas; Oct. 1998
(IAEA-CN-69/EXP2/14)

NIFS-576 S. Murakami, U. Gasparino, H. Idei, S. Kubo, H. Maassberg, N. Marushchenko, N. Nakajima, M. Romé and M Okamoto,
5D Simulation Study of Suprathermal Electron Transport in Non-Axisymmetric Plasmas; Oct. 1998
(IAEA-CN-69/THP1/01)

NIFS-577 S. Fujiwara and T. Sato,
Molecular Dynamics Simulation of Structure Formation of Short Chain Molecules; Nov. 1998

NIFS-578 T. Yamagishi,
Eigenfunctions for Vlasov Equation in Multi-species Plasmas Nov. 1998

NIFS-579 M. Tanaka, A. Yu Grosberg and T. Tanaka,
Molecular Dynamics of Strongly-Coupled Multichain Coulomb Polymers in Pure and Salt Aqueous Solutions; Nov. 1998

NIFS-580 J. Chen, N. Nakajima and M. Okamoto,
Global Mode Analysis of Ideal MHD Modes in a Heliotron/Torsatron System: I. Mercier-unstable Equilibria; Dec. 1998

NIFS-581 M. Tanaka, A. Yu Grosberg and T. Tanaka,
Comparison of Multichain Coulomb Polymers in Isolated and Periodic Systems: Molecular Dynamics Study; Jan. 1999

NIFS-582 V.S. Chan and S. Murakami,

Self-Consistent Electric Field Effect on Electron Transport of ECH Plasmas; Feb 1999

NIFS-583 M Yokoyama, N Nakajima, M. Okamoto, Y Nakamura and M Wakatani,
Roles of Bumpy Field on Collisionless Particle Confinement in Helical-Axis Heliotrons Feb 1999

NIFS-584 T -H Watanabe, T. Hayashi, T Sato, M Yamada and H. Ji,
Modeling of Magnetic Island Formation in Magnetic Reconnection Experiment, Feb 1999

NIFS-585 R Kumazawa, T Mutoh, T Seki, F Shinpo, G Nomura, T Ido, T. Watari, Jean-Marie Noterdaeme and Yangping Zhao,
Liquid Stub Tuner for Ion Cyclotron Heating, Mar 1999

NIFS-586 A. Sagara, M Iima, S Inagaki, N. Inoue, H Suzuki, K Tsuzuki, S. Masuzaki, J Miyazawa, S Morita, Y Nakamura, N Noda, B. Peterson, S Sakakibara, T. Shimozuma, H Yamada, K Akaishi, H. Chikaraishi, H Funaba, O Kaneko, K Kawahata, A Komon, N Ohyabu, O. Motojima, LHD Exp Group 1, LHD Exp. Group 2,
Wall Conditioning at the Starting Phase of LHD; Mar 1999

NIFS-587 T Nakamura and T. Yabe,
Cubic Interpolated Propagation Scheme for Solving the Hyper-Dimensional Vlasov-Poisson Equation in Phase Space; Mar 1999

NIFS-588 W X Wnag, N. Nakajima, S Murakami and M. Okamoto,
An Accurate δf Method for Neoclassical Transport Calculation; Mar 1999

NIFS-589 K Kishida, K. Araki, S Kishiba and K Suzuki,
Local or Nonlocal? Orthonormal Divergence-free Wavelet Analysis of Nonlinear Interactions in Turbulence; Mar. 1999

NIFS-590 K Araki, K. Suzuki, K. Kishida and S Kishiba,
Multiresolution Approximation of the Vector Fields on T^3; Mar 1999

NIFS-591 K. Yamazaki, H Yamada, K.Y.Watanabe, K Nishimura, S Yamaguchi, H Nakanishi, A Komon, H Suzuki, T Mito, H. Chikaraishi, K. Murai, O. Motojima and the LHD Group,
Overview of the Large Helical Device (LHD) Control System and Its First Operation, Apr 1999

NIFS-592 T. Takahashi and Y Nakao,
Thermonuclear Reactivity of D-T Fusion Plasma with Spin-Polarized Fuel, Apr 1999

NIFS-593 H. Sugama,
Damping of Toroidal Ion Temperature Gradient Modes, Apr. 1999

NIFS-594 Xiaodong Li,
Analysis of Crowbar Action of High Voltage DC Power Supply in the LHD ICRF System, Apr 1999

NIFS-595 K. Nishimura, R. Horiuchi and T. Sato,
Drift-kink Instability Induced by Beam Ions in Field-reversed Configurations, Apr 1999

NIFS-596 Y. Suzuki, T-H. Watanabe, T. Sato and T Hayashi,
Three-dimensional Simulation Study of Compact Toroid Plasmoid Injection into Magnetized Plasmas; Apr. 1999

NIFS-597 H. Sanuki, K. Itoh, M Yokoyama, A Fujisawa, K. Ida, S. Toda, S -I Itoh, M Yagi and A. Fukuyama,
Possibility of Internal Transport Barrier Formation and Electric Field Bifurcation in LHD Plasma, May 1999

NIFS-598 S. Nakazawa, N. Nakajima, M Okamoto and N. Ohyabu,
One Dimensional Simulation on Stability of Detached Plasma in a Tokamak Divertor, June 1999

NIFS-599 S. Murakami, N. Nakajima, M. Okamoto and J Nhrenberg,
Effect of Energetic Ion Loss on ICRF Heating Efficiency and Energy Confinement Time in Heliotrons, June 1999

NIFS-600 R. Horiuchi and T. Sato,
Three-Dimensional Particle Simulation of Plasma Instabilities and Collisionless Reconnection in a Current Sheet;; June 1999

NIFS-601 W. Wang, M. Okamoto, N. Nakajima and S. Murakami,
Collisional Transport in a Plasma with Steep Gradients; June 1999

NIFS-602 T. Mutoh, R. Kumazawa, T. Saki, K. Saito, F. Simpo, G. Nomura, T. Watari, X. Jikang, G. Cattanei, H. Okada, K. Ohkubo, M. Sato, S. Kubo, T Shimozuma, H. Idei, Y. Yoshimura, O. Kaneko, Y. Takein, M. Osakabe, Y. Oka, K. Tsumori, A. Komori, H. Yamada, K. Watanabe, S. Sakakibara, M. Shoji, R. Sakamoto, S. Inagaki, J. Miyazawa, S. Morita, K. Tanaka, B.J Peterson, S. Murakami, T. Minami, S. Ohdachi, S. Kado, K. Narihara, H. Sasao, H. Suzuki, K. Kawahata, N. Ohyabu, Y. Nakamura, H. Funaba, S. Masuzaki, S. Muto, K. Sato, T. Morisaki, S. Sudo, Y. Nagayama, T. Watanabe, M. Sasao, K.. Ida, N. Noda, K. Yamazaki, K. Akaishi, A. Sagara, K. Nishimura, T Ozaki, K. Toi, O. Motojima, M. Fujiwara, A. Iiyoshi and LHD Exp. Group 1 and 2,
First ICRF Heating Experiment in the Large Helical Device; July 1999

NIFS-603 P.C. de Vries, Y. Nagayama, K. Kawahata, S. Inagaki, H. Sasao and K. Nagasaki,
Polarization of Electron Cyclotron Emission Spectra in LHD; July 1999

NIFS-604 W. Wang, N. Nakajima, M. Okamoto and S. Murakami,
δf Simulation of Ion Neoclassical Transport; July 1999

NIFS-605 T. Hayashi, N Mizuguchi, T. Sato and the Complexity Simulation Group,
Numerical Simulation of Internal Reconnection Event in Spherical Tokamak; July 1999

NIFS-606 M. Okamoto, N. Nakajima and W. Wang,
On the Two Weighting Scheme for δf Collisional Transport Simulation; Aug. 1999

NIFS-607 O. Motojima, A.A. Shishkin, S. Inagaki, K. Y Watanabe,
Possible Control Scenario of Radial Electric Field by Loss-Cone-Particle Injection into Helical Device: Aug. 1999

NIFS-608 R. Tanaka, T. Nakamura and T. Yabe,
Constructing Exactly Conservative Scheme in Non-conservative Form; Aug. 1999

NIFS-609 H. Sugama,
Gyrokinetic Field Theory; Aug. 1999

NIFS-610 M. Takechi, G. Matsunaga, S. Takagi, K.Ohkuni, K. Toi, M. Osakabe, M. Isobe, S. Okamura, K. Matsuoka, A. Fujisawa, H Iguchi, S. Lee, T. Minami, K. Tanaka, Y. Yoshimura and CHS Group,
Core Localized Toroidal Alfven Eigenmodes Destabilized By Energetic Ions in the CHS Heliotron/Torsatron; Sep. 1999

NIFS-611 K. Ichiguchi,
MHD Equilibrium and Stability in Heliotron Plasmas; Sep. 1999

NIFS-612 Y. Sato, M. Yokoyama, M. Wakatani and V D. Pusovitov,
Complete Suppression of Pfirsch-Schluter Current in a Toroidal l=3 Stellarator; Oct. 1999

NIFS-613 S. Wang, H. Sanuki and H. Sugama,
Reduced Drift Kinetic Equation for Neoclassical Transport of Helical Plasmas in Ultra-low Collisionality Regime; Oct. 1999

NIFS-614 J. Miyazawa, H. Yamada, K. Yasui, S Kato, N., Fukumoto, M. Nagata and T. Uyama,
Design of Spheromak Injector Using Conical Accelerator for Large Helical Device, Nov. 1999

NIFS-615 M. Uchida, A. Fukuyama, K. Itoh, S.-I. Itoh and M Yagi,
Analysis of Current Diffusive Ballooning Mode in Tokamaks; Dec. 1999

NIFS-616 M. Tanaka, A.Yu Grosberg and T. Tanaka,
Condensation and Swelling Behavior of Randomly Charged Multichain Polymers by Molecular Dynamics Simulations; Dec. 1999

NIFS-617 S. Goto and S. Kida,
Sparseness of Nonlinear Coupling; Dec. 1999

NIFS-618 M.M. Skoric, T Sato, A. Maluckov and M.S. Jovanovic,
Complexity in Laser Plasma Instabilities Dec. 1999